

Article

# Evolution of Phase Transition and Mechanical Properties of Ultra-High Strength Hot-Stamped Steel During Quenching Process

Shuang Liu <sup>1,2</sup>, Mujun Long <sup>1,2,\*</sup> , Songyuan Ai <sup>1,2</sup>, Yan Zhao <sup>3,\*</sup>, Dengfu Chen <sup>1,2</sup>, Yi Feng <sup>3</sup>, Huamei Duan <sup>1,2</sup> and Mingtu Ma <sup>3</sup>

<sup>1</sup> State Key Laboratory of Coal Mine Disaster Dynamics & Control, College of Materials Science and Engineering, Chongqing University, Chongqing 400044, China; liushuang666@163.com (S.L.); asy@cqu.edu.cn (S.A.); chendfu@cqu.edu.cn (D.C.); duanhuamei@cqu.edu.cn (H.D.)

<sup>2</sup> Chongqing Key Laboratory of Vanadium-Titanium Metallurgy and New Materials, Chongqing University, Chongqing 400044, China

<sup>3</sup> China Automotive Engineering Research Institute Co. Ltd., Chongqing 401122, China; fengyi@caeri.com.cn (Y.F.); mamingtu@caeri.com.cn (M.M.)

\* Correspondence: longmujun@cqu.edu.cn (M.L.); zhaoyan@caeri.com.cn (Y.Z.); Tel.: +86-135-9431-8151 (M.L.); +86-159-2323-7149 (Y.Z.)

Received: 30 November 2019; Accepted: 14 January 2020; Published: 16 January 2020



**Abstract:** Hot stamping process is widely used in the manufacture of the high strength automotive steel, mainly including the stamping and quenching process of the hot-formed steel. In the hot stamping process, the steel is heated above the critical austenitizing temperature, and then it is rapidly stamped in the mold and the quenching phase transition occurs at the same time. The quenching operation in the hot stamping process has a significant influence on the phase transition and mechanical properties of the hot-stamping steel. A proper quenching technique is quite important to control the microstructure and properties of an ultra-high strength hot-stamping steel. In this paper, considering the factors of the austenitizing temperature, the austenitizing time and the cooling rate, a coupled model on the thermal homogenization and phase transition from austenite to martensite in quenching process was established for production of ultra-high strength hot-stamping steel. The temperature variation, the austenite decomposition and martensite formation during quenching process was simulated. At the same time, the microstructure and the properties of the ultra-high strength hot-stamping steel after quenching at different austenitizing temperature were experimental studied. The results show that under the conditions of low cooling rate, the final quenching microstructure of the ultra-high strength hot-stamping steel includes martensite, residual austenite, bainite and ferrite. With the increase of the cooling rate, bainite and ferrite gradually disappear. While austenitizing at 930 °C, the tensile strength, yield strength, elongation and strength-ductility product of the hot-stamping steel are 1770.1 MPa, 1128.2 MPa, 6.72% and 11.9 GPa%, respectively.

**Keywords:** phase transition; mechanical properties; quenching; ultra-high strength steel

## 1. Introduction

With the rapid development of the lightweight technology in the automobile industry, high-strength automobile steel gradually replaces the original low-strength automobile steel [1,2]. Due to the difficulty of the cold forming technology, hot stamping technology has become the main technology of producing the high-strength automobile steel, which mainly includes the process of austenitizing, quenching and plastic forming [3]. In the hot stamping process, in order to reduce the deformation resistance of the hot-stamped steel at high temperature, it is heated above the critical

austenitizing temperature [4]. After the rapid stamping in the mold, it is quenched at a higher cooling rate, and finally martensite microstructure is obtained, which greatly improves the strength of the hot-formed steel [5]. However, although the whole martensite steel that was obtained after the hot stamping process has a high strength, its toughness is not high, which greatly restricts the application of the hot-stamped steel in automobile field [6]. The toughness and plasticity of the ultra-high strength steel are closely related to the quenching parameters in the hot stamping process, and the appropriate hot stamping process is the basis of the production of the high-quality automobile steel with ultra-high strength [7]. In order to improve the strength and plasticity of the hot stamping steel, it is of great significance to study the phase transition in the quenching process and its influence on the mechanical properties.

Mu et al. [8] studied the influence of the austenitizing temperature, deformation rate and other factors on the temperature variation and mechanical properties of 22MnB5 in quenching process. It was found that the peak stress of hot-stamping steel during deformation increased with the increase of the austenite volume fraction. N. Vu-Bac et al. [9] studied the numerical analysis process of industrial data, and the model can accurately reflect the experimental data in practical application, providing method guidance for the numerical simulation process in industrial production. Wang et al. [10] simulated the quenching process of 22MnB5 under different conditions in the hot stamping process, and found that the final microstructure composition of the hot-stamping steel is closely related to the cooling rate. Xing et al. [11] simulated the quenching process of boron steel in the hot stamping process, and found that the appropriate quenching process increased the tensile strength of the hot-stamping steel by 2.5 times. Although many scholars have done some research on the quenching process of 1500 MPa hot-stamping steel [12–14], further exploration on the phase transition process and the effect of heat treatment on the mechanical properties of ultra-high strength hot-stamping steel are still lacking. Therefore, in order to improve the strength and plasticity of ultra-high strength hot-stamping steel, it is very important to study the phase transition and the mechanical property variation in the hot stamping process.

In this paper, considering the different austenitizing temperature and holding time, the coupled mathematical model of the thermal and phase transition is established for the quenching process of the hot-stamping steel under different cooling rates. The temperature variation and phase transition process of ultra-high strength hot-stamping steel are simulated and studied. The microstructure and mechanical properties of ultra-high strength hot-stamping steel under different quenching conditions are observed and analyzed. The results provide the guidance for the quenching process of the ultra-high strength hot-stamping steel.

## 2. Mathematical Equations

The three-dimensional unsteady heat conduction differential equation is used in the current model to calculate the heat transfer.

$$\rho c \frac{\partial T}{\partial \tau} = \frac{\partial}{\partial x} \left( \lambda \frac{\partial T}{\partial x} \right) + \frac{\partial}{\partial y} \left( \lambda \frac{\partial T}{\partial y} \right) + \frac{\partial}{\partial z} \left( \lambda \frac{\partial T}{\partial z} \right) + \varphi, \quad (1)$$

where,  $T$ ,  $\rho$ ,  $c$ ,  $\tau$  and  $\varphi$  are infinitesimal body temperature in °C, density in Kg/m<sup>3</sup>, specific heat in J/(Kg °C), time in s and per unit time per unit volume of the heat, which is generated by the internal heat source in J/(m<sup>3</sup> s), respectively.  $\lambda$  is thermal conductivity in W/(m K). The physical properties of the steel are shown in Figure 1.

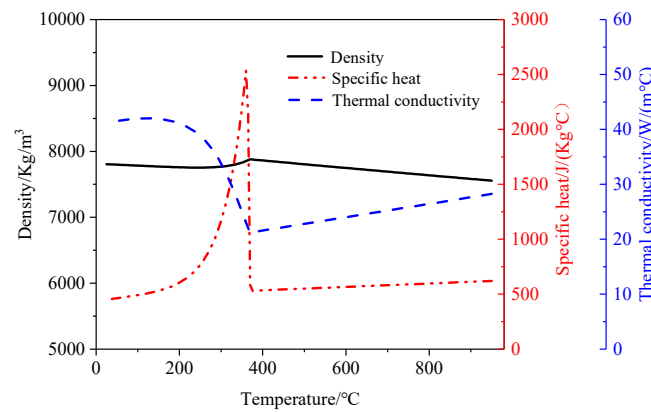


Figure 1. Physical properties of the steel.

The equation between heat transfer coefficient and temperature is as follows.

$$\phi = \eta A (T_A - T_w), \quad (2)$$

where,  $\phi$ ,  $\eta$ ,  $A$ ,  $T_A$  and  $T_w$  are heat transfer rate in W, heat transfer coefficient in  $W/(m^2 \cdot ^\circ C)$ , heat transfer area in  $m^2$ , average steel plate temperature in  $^\circ C$  and mold temperature in  $^\circ C$ , respectively.

The phase transition model was established to simulate the transition of austenite into martensite, bainite, ferrite and pearlite. The reaction equation of austenite decomposition can be described as follows.

$$\frac{dX_i}{d\tau} = f(G)f(X_i)f(T)f(V), \quad (3)$$

where,  $f(G)$  is the influence function of the austenite grain size in the transition process, and  $f(X_i)$  is the influence function of the current phase content on the microstructure transition.  $f(T)$  is the influence function of the temperature on the transition, and  $f(V)$  is the influence function of the alloy elements on the transition rate of each phases.  $G$  is the austenite grain size, and  $X_i$  is the volume fraction of each phases at the current time, which is dimensionless.  $T$  is the temperature in  $^\circ C$ , and  $V$  is the transition rate in %/s. Detailed description of the equations can be found in the references [1,15–18].

The influence function of the austenite grain size in the transition process is as follows.

$$f(G) = 2^{(G-1)/2}, \quad (4)$$

where,  $G$  is constant, and the value is 8. In this study, it is assumed that this parameter remains unchanged during the cooling process [1,15].

The influence function of the current phase content on the microstructure transition is as follows.

$$f(X_i) = \frac{(X_i)^{2(1-X_i)/3}(1-X_i)^{2X_i/3}}{Y}, \quad (5)$$

$$Y = \exp(C_b X_i^2), \quad (6)$$

$$C_b = 1.9C + 2.5Mn + 9Ni + 1.7Cr + 4Mo - 2.6, \quad (7)$$

where,  $Y$  is the phase influence factor, and  $y = 1$  for ferrite and pearlite.  $C_b$  is the bainite delayed formation factor, which is dimensionless, and it depends on the alloy content in the metal.

The influence function of the temperature on phase transition is as follows.

$$f(T) = (T_a - T)^n \exp(-Q_i/RT), \quad (8)$$

where,  $(T_\alpha - T)$  is the degree of supercooling, and  $T_\alpha$  is the starting temperature of each phase transition ( $^\circ\text{C}$ ).  $T$  is the current temperature ( $^\circ\text{C}$ ), and for ferrite and pearlite  $n = 3$ , and for bainite  $n = 2$ .  $Q_i$  is the diffusion activation energy ( $\text{J}/(\text{Kg mol})$ ), and  $R$  is the general gas constant.

The influence function of the alloy elements on the transition rate of each phases is as follows.

$$f(V_{\text{ferrite}}) = (59.6Mn + 1.45Ni + 67.7Cr + 244Mo + K_f B)^{-1}, \quad (9)$$

$$f(V_{\text{pearlite}}) = \{[1.79 + 5.42(Cr + Mo + 4MoNi) + K_p B]D\}^{-1}, \quad (10)$$

$$D = \frac{1}{\exp(-27500/RT)} + \frac{0.01C + 0.52Mo}{\exp(-37000/RT)}, \quad (11)$$

$$f(V_{\text{bainite}}) = [10^{-4}(2.34 + 10.1C + 3.8Cr + 19Mo)]^{-1}, \quad (12)$$

where,  $K_f$  and  $K_p$  are constant, and the value is  $1.9 \times 10^5$  and  $3.1 \times 10^3$ , respectively.

In this paper, according to the steel composition, the phase transition parameters of the hot-stamping steel were calculated by JMatPro software (Version 7.0, JMatPro, Sente Software, Guildford, UK), and then the relevant parameters were directly imported into DEFORM software (Version 10.2, Deform, Scientific Forming Technologies Corporation, Columbus, OH, USA), and the coupled model of thermal and phase transition was established to simulate the quenching process of ultra-high strength hot-stamping steel.

### 3. Research Approaches

Firstly, the quenching transition process in the hot stamping process was simulated by DEFORM software. The temperature variation and phase transition in the process of quenching were simulated under the conditions: austenitizing temperature at  $930^\circ\text{C}$ , austenitizing time in 5 min and the average cooling rate at  $40^\circ\text{C}/\text{s}$ . The model grid and results extraction method are shown in Figure 2. The number of the model nodes was 39865, and the number of the units was 150,000. The heat transfer coefficient at the sample surface was  $1300 \text{ W}/(\text{m}^2 \cdot ^\circ\text{C})$ . The initial phase microstructure of the sample was austenite with volume fraction of 1.0. The parameters used in the simulation are listed in Table 1. The steel used for quenching was ultra-high strength hot-stamping steel, and its composition is shown in Table 2. The steel we used is 28MnB5 hot-formed steel produced by a steel plant in China. The steel was a 1800 MPa grade automotive hot-formed steel with a thickness of 1.5 mm, which can be used for making anti-collision beams. The phase transition parameters of the steel were calculated by JMatPro software, and then were imported into DEFORM software for calculation. The same method was used to simulate the phase transition process with the average cooling rate of  $10^\circ\text{C}/\text{s}$  and  $25^\circ\text{C}/\text{s}$  with austenitizing temperature at  $930^\circ\text{C}$  and austenitizing time in 5 min. The surface heat transfer coefficients corresponding to  $10^\circ\text{C}/\text{s}$  and  $25^\circ\text{C}/\text{s}$  were  $340 \text{ W}/(\text{m}^2 \cdot ^\circ\text{C})$  and  $850 \text{ W}/(\text{m}^2 \cdot ^\circ\text{C})$ , respectively. Then the simulation results of a, b, c, d and e on the cross section of the sample were compared and analyzed.

**Table 1.** The parameters used in the simulation.

Austenitizing temperature	$930^\circ\text{C}$
Austenitizing time	5 min
Heat transfer coefficient	$1300 \text{ W}/(\text{m}^2 \cdot ^\circ\text{C})$
Initial austenite content	1
Mold temperature	$150^\circ\text{C}$

**Table 2.** The composition of ultra-high strength hot-stamping steel.

C	Mn	Si	Al	B	Cr	Cu	Nb	Ti	V	Mo
0.28	1.5	0.25	0.042	0.003	0.24	0.0061	0.053	0.0263	0.0033	0.0032

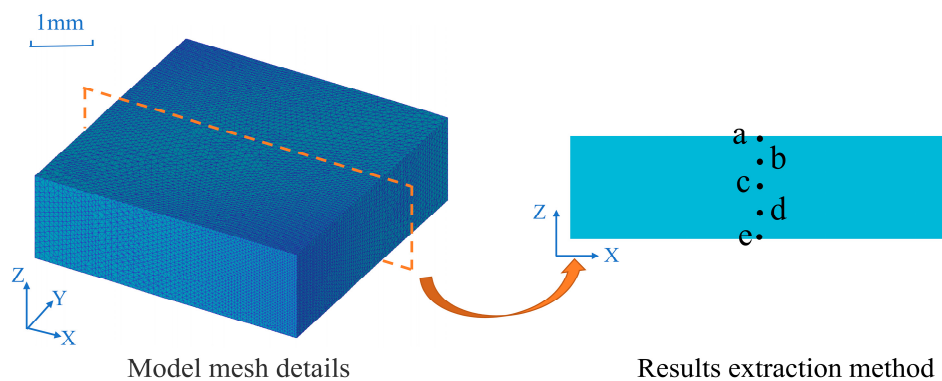


**Figure 2.** Grid model and analysis point location.

In order to verify the accuracy of the simulation results and study the mechanical properties of the steel under different quenching conditions, the microstructure, tensile strength, yield strength, hardness and elongation of the hot-stamping steel after quenching under different austenitizing temperatures were studied in laboratory. Firstly, the hot-stamping steel sheet was cut into  $1.5 \text{ mm} \times 5.0 \text{ mm} \times 5.0 \text{ mm}$  cube and A<sub>50</sub> standard sample. Secondly, the samples were austenitizing in the muffle furnace at 840 °C, 900 °C, 930 °C, 960 °C and 990 °C for 5 min, then were transferred to the mold and cooled to 150 °C at a cooling rate of 40 °C/s, prior to air cooling to room temperature. The samples after heat treatment were polished with the water abrasive paper of 400#, 600#, 1000# and 2000#. With each change of abrasive paper, the specimen was rotated 90° so that it was perpendicular to the old scratch, and finally the scratch on the steel surface disappeared completely. Afterwards, the steel samples were polished by diamond polishing agent and nylon polishing cloth, and then the polished steel samples were put into 4% nitric acid alcohol solution to corrode for 10 s. Finally, the samples were observed by metallographic microscope. The strength of the hot-stamped steel was measured by the SANS CMT5035 tensile testing machine (MTS, Shenzhen, China) with a strain rate of 5 mm/min. Before the test, the oxide layer and oil stains on the sample surface were polished by using 60# sandpaper to prevent slip at the clamping end during the stretching process, and then the Vickers hardness of the hot-stamped steel was measured by microhardness machine. In order to avoid the data fluctuation caused by the experimental error, each group of samples was measured three times, and the average value was calculated as the final result.

## 4. Results and Discussion

### 4.1. Simulation of the Phase Evolution in Quenching Process

#### 4.1.1. Temperature Homogenization

Figures 3 and 4 show the temperature variation during the quenching process at an average cooling rate of 40 °C/s. With the increase of the quenching time, the temperature of the hot-stamping steel decreased gradually. The quenching process was a continuous non-constant speed cooling. At the early stage of the quenching, the cooling rate was larger than 40 °C/s since the temperature difference between the steel and the mold was large. The cooling rate decreased with quenching time as the temperature difference between the steel and the mold decreased gradually. The cooling rate was lower than 40 °C/s at final stage of quenching.

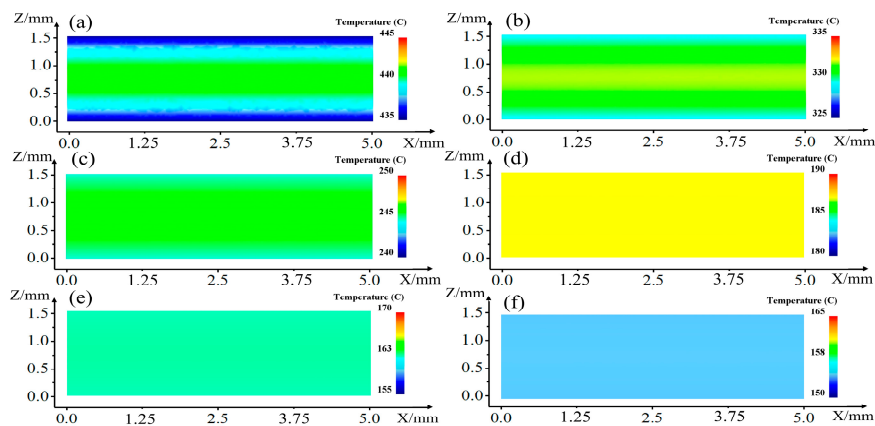


**Figure 3.** Temperature distribution under different quenching time: (a) 3 s, (b) 6 s, (c) 9 s, (d) 12 s, (e) 15 s and (f) 18 s.

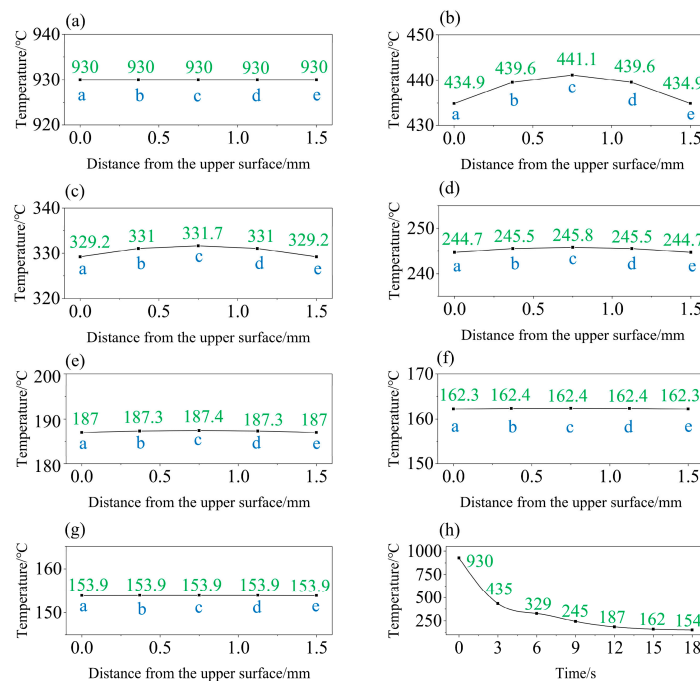
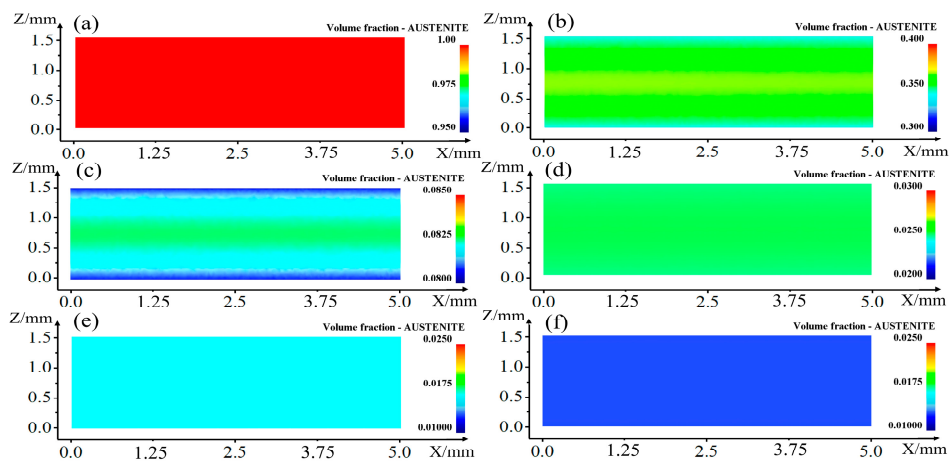


**Figure 4.** Temperature variation during quenching process: (a) 0 s, (b) 3 s, (c) 6 s, (d) 9 s, (e) 12 s, (f) 15 s, (g) 18 s and (h) temperature variation with time at location a.

As shown in Figures 3a and 4b, the temperature of the hot-stamping steel sample increased gradually from outside to inside at the quenching time of 3 s. The temperature of location c in the center was 441.15 °C and the temperature of location a on the surface was 434.86 °C. The temperature on the surface was around 10 °C lower than that in the center because of the strong heat transfer between the sample surface and the die. In addition, the surface temperature drop rate was greater than that inside the hot-stamping steel. When the quenching time reached 12s, the temperature of location c in the center of the sample was 187.41 °C, and the temperature of location a on the surface was 186.98 °C, the temperature distribution of the sample tended to be uniform, indicating that the hardenability of the hot-stamping steel was good to meet the requirements of the existing process. In the whole quenching process, The temperature drop rate in the first three seconds was the fastest, and the surface temperature of the sample dropped rapidly from 930 to 435 °C. Then the cooling rate came down and the temperature of the sample gradually decreased as the quenching going on.

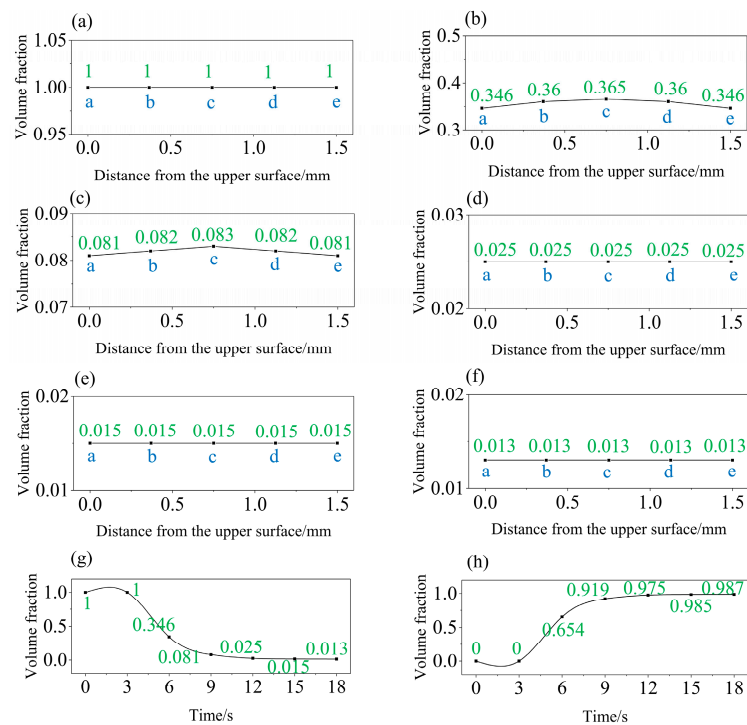
#### 4.1.2. Phase Transition during Quenching

Figure 5 shows the volume fraction variation of the austenite and martensite with time during the quenching. With the increase of the quenching time, the austenite transforms into martensite gradually. At the first 3 s, the sample did not reach the critical temperature of martensite transition, and the phase stays as austenite, as shown in Figure 5a. When the quenching time was 6 s, the transition from austenite to martensite began. Since the surface temperature of the sample was lower than the internal temperature, the decomposition proportion of the austenite on the surface of the sample was higher than that inside, as shown in Figure 5b. It could be seen from Figure 5c that when the quenching time reached 9 s, the volume fraction of the residual austenite was less than 0.1. Since the temperature of the sample surface was lower than that inside the sample, the amount of the austenite decomposition on the surface was higher than that inside the sample, and there were more residual austenite inside the sample than that on the surface. When the quenching time reached 12 s, the distribution of the retained austenite was relatively uniform, and the content of the retained austenite on the surface was almost the same as that in the interior, as shown in Figure 5d.



**Figure 5.** Austenite volume fraction and distribution during quenching process: (a) 3 s, (b) 6 s, (c) 9 s, (d) 12 s, (e) 15 s and (f) 18 s.

Figure 6 shows the variation of the phase volume fraction with quenching time at a, b, c, d and e locations. In the first 3 s, the volume fraction of the austenite was 1.0, indicating that the austenite did not start to decompose. When the quenching time was 6 s, the volume fraction of the austenite at a, b, c, d and e was 0.346, 0.36, 0.365, 0.36 and 0.346, respectively. It could be seen from Figure 6g,h that the transition rates of the austenite decomposition and martensite formation were the largest in around 21.8%/s between 3 and 6 s, and then decreased gradually after 6 s. When the quenching time was 9 s, the volume fraction of the austenite at locations a, b, c, d and e was 0.081, 0.082, 0.083, 0.082 and 0.081, respectively, which shows that austenite was still decomposing fast relatively during the quenching from 6 to 9 s. When the quenching time reached 12 s, the volume fraction of austenite at locations a, b, c, d and e was 0.025, showing that the distribution of austenite was uniform and the decomposition rate of austenite slowed down to a low level between 9 and 12 s. The residual austenite continued to decompose slowly. After quenching for 18 s, the volume fraction of austenite was 0.013 for the sample. In the quenching process, austenite was gradually decomposed and martensite was gradually formed. From Figure 6g,h, it can be seen that the decomposition rate of the austenite and the formation rate of the martensite are the fastest between 3 and 9 s, and then the decomposition rate of the austenite and the formation rate of the martensite slowed down gradually. The retained austenite content of the hot-stamping steel was 1.3% and the martensite content was 98.7% when it was quenched to the die temperature.



**Figure 6.** Variation of the phases volume fractions during quenching process: (a) austenite fraction at 3 s, (b) austenite fraction at 6 s, (c) austenite fraction at 9 s, (d) austenite fraction at 12 s, (e) austenite fraction at 15 s, (f) austenite fraction at 18 s, (g) austenite fraction versus time at location a and (h) martensite fraction versus time at location a.

#### 4.1.3. Effect of Cooling Rate on Phase Transition

Figure 7 shows the phase compositions of the steel after quenching at different cooling rates. With the increase of the cooling rate, the content of the residual austenite tended to increase, and the phases of bainite and ferrite disappeared. When the cooling rate was  $10\text{ }^{\circ}\text{C/s}$ , the main phase was martensite in 98.7%, and the residue austenite was 1.2%, and the other phases such as bainite and ferrite were 0.1%. When the cooling rate increased to  $25\text{ }^{\circ}\text{C/s}$ , the volume fraction of the martensite was 98.8%, and the content of the austenite was 1.2%. The other phases disappeared. When the cooling rate was  $40\text{ }^{\circ}\text{C/s}$ , the volume fractions of the martensite and the austenite were 98.7% and 1.3%, respectively. The results indicate that with the increase of the cooling rate, ferrite and bainite were inhibited and austenite tended to increase. Thus, it is beneficial to improve the strength and the plasticity of the current hot-stamping steel with ultra-high strength. In the actual hot-stamped process, the cooling rate was  $40\text{ }^{\circ}\text{C/s}$ . According to the calculation results, there were more austenite in the cooling rate at  $40\text{ }^{\circ}\text{C/s}$ , so the cooling rate at  $40\text{ }^{\circ}\text{C/s}$  could meet the demand of the actual production process.

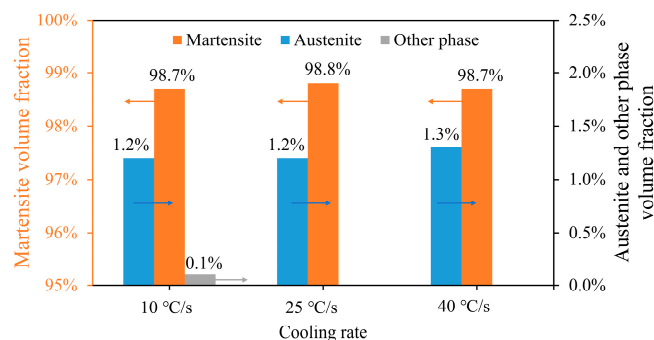


**Figure 7.** Phase compositions of the steel after quenching at different cooling rates.

#### 4.2. Experimental Analysis on the Steel after Quenching

Austenitizing temperature and time are important parameters in the quenching process of hot-formed steel, which directly affect the mechanical properties of the final product. If the austenitizing temperature is too low, the microstructure after quenching will contain more ferrite, which reduces the strength of the hot-formed steel and produces uneven stress in the process of stamping. If the austenitizing temperature is too high and the time is too long, the grain will grow quickly, which reduces the mechanical properties of the hot-formed steel. Therefore, proper austenitizing temperature and time are the preconditions for obtaining high mechanical properties of hot formed steel.

##### 4.2.1. Effect of Austenitizing Temperature on the Microstructure

Figure 8 shows the microstructures of the hot-stamping steel after quenching under different austenitizing temperatures. In the quenching experiment, the holding time was 5 min, and the cooling rate was 40 °C/s. The initial microstructure of the hot-stamping steel was mainly ferrite and pearlite. As the results indicate, all the final microstructure contained a large amount of martensite, providing a strong guarantee for the high strength performance of the hot-stamping steel. With the increase of austenitizing temperature, the martensite grain gradually became coarser, which might reduce the strength and the service performance of the hot-stamping steel. Therefore, it is of great significance to select the appropriate austenitizing temperature for the improvement of the comprehensive performance of the hot-stamping steel. By comparing the microstructure in Figure 8d with the simulation results in Figure 6, both the simulation results and the experimental results show that the final phase composition of the hot-stamping steel after quenching was mostly martensite, verifying the accuracy of the simulation results.

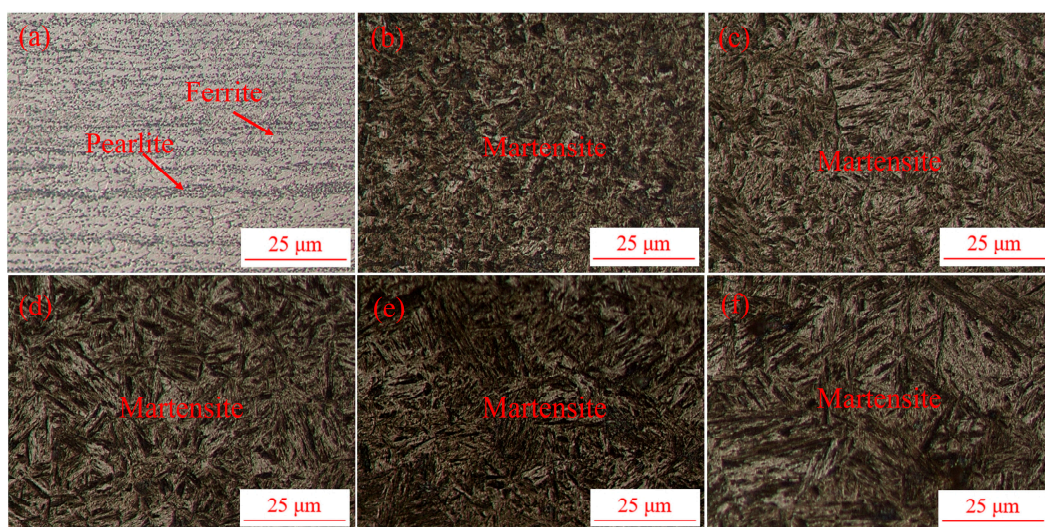


**Figure 8.** Microstructures of the hot-stamping steel after different austenitizing temperatures: (a) original sample, (b) 840 °C, (c) 900 °C, (d) 930 °C, (e) 960 °C and (f) 990 °C.

##### 4.2.2. Effect of Austenitizing Temperature on the Mechanical Properties

Before the austenitizing and quenching process, the tensile strength, yield strength, hardness, elongation and strength-ductility product of the hot-stamping steel were 528.9 MPa, 370.5 MPa, 156.6 Hv, 29.8% and 15.76 GPa%, respectively. After the austenitizing and quenching process, the properties of the hot-stamping steel were improved significantly, as indicated in Figure 9. When the austenitizing temperatures were 840 °C, 900 °C, 930 °C, 960 °C and 990 °C, the tensile strengths of the hot-stamping steel were 1831.2 MPa, 1781.9 MPa, 1770.1 MPa, 1722.9 MPa and 1707.4 MPa, respectively. The hardness were 539.5 Hv, 526.8 Hv, 527 Hv, 530.6 Hv and 529.2 Hv, respectively. The tensile strength and hardness of the hot-stamping steel decreased with the increase of austenitizing temperature. At a

higher austenitizing temperature, longer time is needed for quenching at the same cooling rate, and then it is easier for the C in martensite to precipitate and form carbide, resulting in reduction of strength of the hot-stamping steel [19]. Under the austenitizing temperatures of 840 °C, 900 °C, 930 °C, 960 °C and 990 °C, the yield strength were 1190.4 MPa, 1116 MPa, 1128.2 MPa, 1061.8 MPa and 1067.4 MPa, respectively. The yield strength decreased with increasing austenitizing temperature. This was caused by the gradual coarseness of the martensitic grains, as shown in Figure 8. Figure 9b shows the effect of the austenitizing temperature on the elongation and the strength-ductility product of the hot-stamping steel. The elongation and the strength-ductility product decrease with the increase of austenitizing temperature. These were also the results of the coarseness of the martensite grains at higher austenitizing temperature. At austenitizing temperature of 840 °C, the elongation and strength-ductility product were 7.5% and 13.73 GPa%, respectively, indicating that 840 °C would be the optimal hot stamping temperature. However, the heat loss and 90 °C temperature drop of the samples during moving from the austenitizing furnace to the die should be considered. Thus, 930 °C would be the optimal austenitizing temperature for the hot-stamped steel, and the steel will drop to 840 °C after transferring to the die.

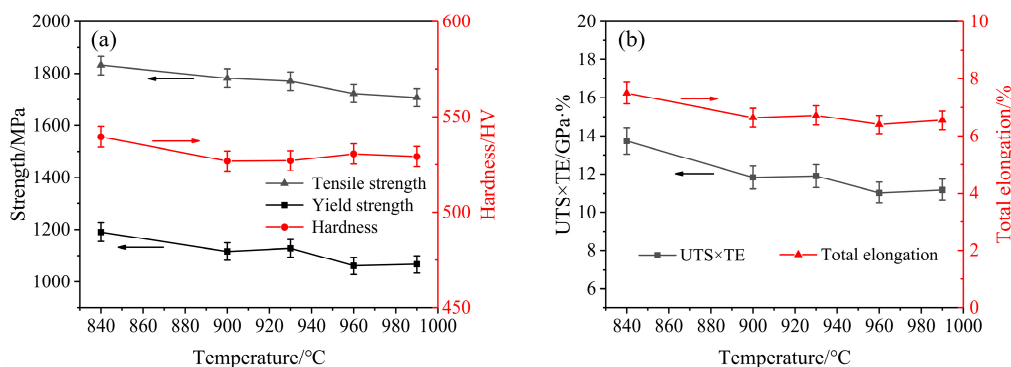


**Figure 9.** The variation of the mechanical properties after different austenitizing temperatures: (a) Strength varies with temperature, (b) Strength-ductility product and total elongation vary with temperature.

Grain refinement can improve the strength of hot-formed steel [20]. When the austenitizing temperature was 840 °C, the tensile strength and elongation of the hot-formed steel were higher than those under other temperature conditions. This is because the austenitizing temperature is relatively low, and the time of quenching to mold temperature is short, and the martensite size is relatively small, as shown in Figure 8b. The quenching microstructure of the hot-formed steel is generally martensite and austenite. With the increase of martensite content, the strength of the hot-formed steel increases gradually but the plasticity decreases, which greatly restricts the application of the high-strength hot-formed steel in automobile field. The presence of a small amount of austenite after quenching can improve the plasticity of the hot-formed steel. In order to ensure that the hot-formed steel has a certain plasticity under high strength condition, the hot formed steel needs to have a small amount of austenite. The martensite and austenite contents in the hot-formed steel after quenching are determined by the quenching conditions, so it is of great engineering significance to directly study the variations in the mechanical properties of the hot-formed steel under different quenching conditions for the research and development of the hot-formed steel with higher strength.

## 5. Conclusions

In this paper, a coupled model of heat transfer and phase transition was established to investigate the temperature variation, phase transition of the ultra-high strength steel under different hot stamping conditions, as well as experimental characterization on the microstructures and mechanical properties. Conclusions are as follows:

(1) The quenching process is a continuous non-constant cooling process. The distributions of temperature and phases became uniform after 12 s at the cooling rate of 40 °C/s.

(2) The higher cooling rate was beneficial to obtain the “martensite + residual austenite” microstructure. As the cooling rate increased to 25 °C/s, the ferrite and bainite disappeared.

(3) With the increase of the austenitizing temperature, the martensite becomes coarser and the tensile strength, yield strength, hardness, elongation and strength-ductility product decreased. The tensile strength, yield strength, hardness, elongation and strength-ductility product under austenitizing temperature of 840 °C were 1831.2 MPa, 1190.4 MPa, 539.5 Hv, 7.5% and 13.73 GPa%, respectively.

**Author Contributions:** Conceptualization, S.L. and M.L.; methodology, M.L.; software, S.L.; validation, S.L. and S.A.; formal analysis, S.L. and M.L.; investigation, S.L., M.L., Y.Z., D.C., Y.F., H.D. and M.M.; writing—original draft preparation, S.L.; writing—review and editing, M.L.; visualization, S.L.; supervision, M.L. All authors have read and agreed to the published version of the manuscript.

**Funding:** This work is funded by the Natural Science Foundation of China (grant numbers U1960113, 51874059, U1564203 and 51874060) and the Natural Science Foundation of Chongqing (grant numbers cstc2018jszx-cyzdX0076 and cstc2018jcyjAX0647).

**Acknowledgments:** This work is supported financially by the Natural Science Foundation of China (NSFC, Project No. U1960113, 51874059, U1564203 and 51874060) and the Natural Science Foundation of Chongqing (Project No. cstc2018jszx-cyzdX0076 and cstc2018jcyjAX0647). The authors thank the members of Laboratory of Metallurgy and Materials, Chongqing University, for the support of this work.

**Conflicts of Interest:** The authors declare no conflict of interest.

## References

- Zhang, P.; Zhu, L.; Xi, C.; Luo, J. Study on Phase Transformation in Hot Stamping Process of USIBOR®1500 High-Strength Steel. *Metals* **2019**, *9*, 1119. [\[CrossRef\]](#)
- Tang, Z.; Gu, Z.; Jia, L.; Li, X.; Zhu, L.; Xu, H.; Yu, G. Research on lightweight design and indirect hot stamping process of the new ultra-high strength steel seat bracket. *Metals* **2019**, *9*, 833. [\[CrossRef\]](#)
- Bao, L.; Zhang, H.J. The research and development of hot stamping forming technology and production line in view of high strength steel plate. *Appl. Mech. Mater.* **2013**, *422*, 75–79. [\[CrossRef\]](#)
- Mu, Y.H.; Wang, B.Y.; Zhou, J.; Huang, X.; Li, J.L. Influences of hot stamping parameters on mechanical properties and microstructure of 30MnB5 and 22MnB5 quenched in flat die. *J. Cent. South Univ.* **2018**, *25*, 736–746. [\[CrossRef\]](#)
- Zhang, P.; Wang, G.; Pan, C.C.; Ren, X.Q. Microstructure and mechanical properties of 22MnB5 hot stamping part. *Adv. Mater. Res.* **2014**, *1063*, 65–68. [\[CrossRef\]](#)
- Sun, L. *Study on Microstructure and Properties of Hot Forming Steel Based on Ultra-Refinement of Austenite Grain*; Harbin Institute of Technology: Harbin, China, 2015.
- Liang, J.; Zhao, Z.; Sun, B.; Lu, H.; Liang, J.; He, Q.; Chen, W.; Tang, D. A novel ultra-strong hot stamping steel treated by quenching and partitioning process. *Mater. Sci. Technol.* **2018**, *34*, 2241–2249. [\[CrossRef\]](#)
- Mu, Y.; Zhou, J.; Wang, B.; Wang, Q.; Chiotti, A.; Bruschi, S. Numerical simulation of hot stamping by partition heating based on advanced constitutive modelling of 22MnB5 behaviour. *Finite Elem. Anal. Des.* **2018**, *147*, 34–44. [\[CrossRef\]](#)
- Vu-Bac, N.; Lahmer, T.; Zhuang, X.; Nguyen-Thoi, T.; Rabczuk, T. A software framework for probabilistic sensitivity analysis for computationally expensive models. *Adv. Eng. Softw.* **2016**, *100*, 19–31. [\[CrossRef\]](#)
- Wang, W.; Liu, Y.; Wen, P.; Tong, J. Numerical simulation on the shape of stamping part about hot forming and quenching. *Appl. Mech. Mater.* **2013**, *328*, 450–456. [\[CrossRef\]](#)
- Xing, Z.; Bao, J.; Yang, Y. Numerical simulation of hot stamping of quenchable boron steel. *Mater. Sci. Eng. A* **2009**, *499*, 28–31. [\[CrossRef\]](#)
- Venturato, G.; Novella, M.; Bruschi, S.; Ghiotti, A.; Shivpuri, R. Effects of phase transformation in hot stamping of 22MnB5 high strength steel. *Procedia Eng.* **2017**, *183*, 316–321. [\[CrossRef\]](#)
- Xu, L.; Zhao, G.; Pan, L.; Du, W.W. Research on the effects of hot stamping process parameters on mechanical property for U-shape part. *Key Eng. Mater.* **2016**, *693*, 863–871. [\[CrossRef\]](#)
- Abdulhay, B.; Bourouga, B.; Dessain, C.; Brun, G.; Wilsius, J. Experimental study of heat transfer in hot stamping process. *Int. J. Mater. Form.* **2009**, *2*, 255–257. [\[CrossRef\]](#)

15. Zhuang, W.; Xie, D.; Tian, Y.; Wandong, Y.U. Numerical simulation of hot forming of high-strength steel based on damage-phase transformation constitutive model. *J. Jilin Univer. Eng. Technol. Ed.* **2015**, *45*, 1206–1212.
16. Zhu, B.; Zhang, Y.S.; Li, J.; Wang, H.; Ye, Z.C. Simulation research of hot stamping and phase transition of automotive high strength steel. *Mater. Res. Innov.* **2011**, *15*, 426–430. [[CrossRef](#)]
17. Cai, Y.; Li, W.; Li, G. Simulation and experiment research of phase transformation on the hot stamping of 22MnB5 high strength steel. *Mater. Res. Innov.* **2014**, *18*, S2509–S2514. [[CrossRef](#)]
18. AKerstrom, P.; Oldenburg, M. Austenite decomposition during press hardening of a boron steel-Computer simulation and test. *J. Mater. Process. Technol.* **2006**, *174*, 399–406. [[CrossRef](#)]
19. Liang, J. *Strengthen-Toughening Mechanism and Application Technology of 2000MPa Grade Hot Stamping Steel*; University of Science & Technology Beijing: Beijing, China, 2019.
20. Liu, H. *Study on High Strength and Elongation Steels Treated by Hot Deformation & QP Process*; Shanghai Jiaotong University: Shanghai, China, 2011.



© 2020 by the authors. Licensee MDPI, Basel, Switzerland. This article is an open access article distributed under the terms and conditions of the Creative Commons Attribution (CC BY) license (<http://creativecommons.org/licenses/by/4.0/>).